Migration of Ionophores and Salts through a Water−Chloroform Liquid−Liquid Interface: Molecular Dynamics−Potential of Mean Force Investigations

M. Lauterbach, E. Engler, N. Muzet, L. Troxler, and G. Wipff*

Laboratoire MSM, Institut de Chimie, 4, rue B. Pascal, 67 000 Strasbourg, France

Received: September 8, 1997; In Final Form: October 3, 1997[⊗]

We report a theoretical study on the liquid−liquid interfacial behavior of the species involved in the extraction of Cs^+ by a calix[4]arene-crown6 ionophore (L): the free Cs^+ Pic^- and Cs^+ Cl^- salts, the LCs^+ and LCs^+ Pic^- complexes, and uncomplexed L. Based on molecular dynamics simulations, we calculated the free energies changes for migration from the interface into the aqueous and the organic phases, respectively. For free L and for the LCs^+ complex, with or without Pic^- counterion, an energy minimum is found close to the interface, on the chloroform side, showing that these species behave as surfactants. This contrasts with the uncomplexed Cs^+, which diffuses spontaneously from the interface to water and displays no energy minimum. A remarkable counterion effect is found with Pic^- which displays a high affinity for the interface, while Cl^- prefers the bulk aqueous phase. The questions of ion extraction by ionophores, counterions, concentration and synergistic effects in assisted cation transfer through the liquid−liquid interface between immiscible liquids are discussed from the interfacial point of view.

Introduction

The transfer of ions across the interface between water and an immiscible organic solvent, facilitated by ionophores, represents an important contemporary issue in physical chemistry.[1−5] Compared to the many studies concerning ion recognition in complexation and transport processes,[6] relatively few studies have been devoted to the question on what happens at the liquid−liquid interface.[7] Little is known about the precise mechanism and dynamics of assisted transfer and, in particular, about the role and microscopic structure of the interface where the extraction reactions may take place. Interfaces have unique chemical and physical properties, which may influence chemical reactivity[8] and complexation selectivity in ways that are different from those in bulk liquids. Moreover, the surface and properties of the interface at rest may differ from the ones in liquid−liquid extraction or transport systems which are vigorously shaken or agitated.

As far as the mechanism of carrier assisted ion transport is concerned, indirect information comes from models used to interpret kinetic data.[9] In the case of static interfaces, thermodynamical characterization comes from surface tension measurements[10,11] and from electrochemical[2,12−14] studies on assisted ion transfer across the organic solvent−water interface, which have been carried out for a variety of ions, solvent systems and carriers. Spectroscopic techniques such as nonlinear optical second harmonic generation and the related IR sum frequency generation,[15] X-ray and neutron specular reflectivity[16] and fluorescence depolarization spectroscopy[17] have been applied to liquid interfaces, but detailed structural information related to ion crossing are still scarce.[18]

Information on the microscopic level can be obtained by molecular dynamics (MD) or Monte Carlo simulations.[19] The first studies on the liquid−liquid interface between Lennard-Jones liquids[20] were followed by simulations of solute free interfaces between water and organic solvents[21] and of water−lipid interfaces.[22] Simulations of solutes at water-vapor[23−25] and at water−liquid interfaces[26,27] reveal a considerable amount of information on the structure and function of aqueous interfaces. As far as ionic solutions are concerned, the question of the double layer structure of ions at the "ITIES" (Interface between two immiscible electrolyte solutions)[28] and the ion transfer across water−liquid interfaces[29] have also been addressed computationally. In relation to assisted ion extraction, we have studied macrocyclic extractant molecules such as crown ethers, calixarene derivatives, the [222]-cryptand, valinomycin, and acyclic ligands such as CMPO's, podants, TBP and their cation complexes at the chloroform-water interface.[30−36] These species are more soluble in the organic phase than in water. However, when the simulation started with the solutes at the interface or in bulk chloroform, the latter did not migrate to chloroform, but adsorbed like surfactants on the chloroform side of the interface. On the other hand, when the uncomplexed Cs^+ Pic^- and Cs^+ Cl^- salts were placed initially at the interface, Cs^+ and Cl^- moved into bulk water, while the Pic^- anion remained adsorbed at the interface.[31,34,36]

In this paper we investigate the structural and energetic features of ion-assisted transfer, based on the one-dimensional free energy profiles for migration from the interface into the chloroform and water phases, respectively. We consider species involved in the extraction of Cs^+ by a calixarene ligand L (L = 1,3 alternate form of 1,3-dimethoxy-calix[4]crown-6; see Figure 1), of particular interest in the context of Cs^+ removal from nuclear waste solutions.[37] A series of consistent PMF (potential of mean force [38]) calculations were performed on the migration of L free and of its LCs^+ inclusion complex. To address the role of counterions, we also simulated the LCs^+Pic^- complex, with the picrate counterion, widely used in ion extraction experiments.[39] The results are compared to those obtained after free MD simulations at the chloroform-water interface, reported previously.[31,32] In addition, PMFs were calculated for the unassisted ion transfer of Cs^+ with two

[⊗] Abstract published in *Advance ACS Abstracts,* December 1, 1997.

S1089-5647(97)02939-8 CCC: $15.00
Published on Web 01/01/1998

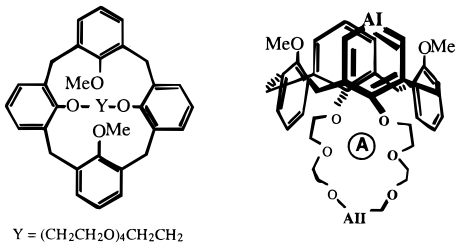

Figure 1. The L ligand, with definition of atoms used for the PMF calculations: A = Cs^+ for the LCs^+ and LCs^+ Pic^- complexes; **AI** or **AII** for L uncomplexed.

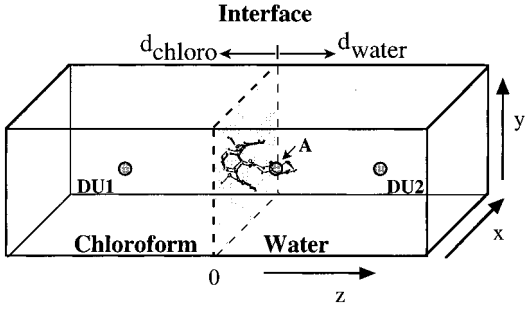

Figure 2. Schematic representation of the solvent boxes and definition of parameters used for the PMF simulations.

different counterions, Cs^+Pic^- and Cs^+Cl^-, for purposes of comparison. The spherical Cl^- anion is hydrophilic, while the flat Pic^- anion, which displays an hydrophilic periphery and two hydrophobic faces can be considered as amphiphilic.[40]

Methods

Representation of the System. We used the modified AMBER4.1 software[41] with the following representation of the potential energy:

$$U = \sum_{\text{bonds}} K_r (r - r_{\text{eq}})^2 + \sum_{\text{angles}} K_\theta (\theta - \theta_{\text{eq}})^2 + \sum_{\text{dihedrals}} \sum_n V_n(1 + \cos n\phi) + \sum_{i<j} (q_i q_j / R_{ij} - 2\epsilon_{ij}(R_{ij}^*/R_{ij})^6 + \epsilon_{ij}(R_{ij}^*/R_{ij})^{12})$$

The bonds and bond angles are treated as harmonic springs and a torsional term is associated to the dihedral angles. The interaction between atoms separated by at least three bonds are described within a pairwise additive scheme by a 1-6-12 potential. Parameters for the solutes were taken from the AMBER force field[42] and our previous studies on these molecules in pure homogeneous solvents.[31,32] The atomic charges on L are given in ref 31 and were used without special scaling factor for 1−4 interactions. The Pic^- anion is described in ref 40. For the solvent, we used the TIP3P model for water[43] and the OPLS model for chloroform,[44] where CH is represented in the united atom approximation. All C−H, O−H, H···H, C−Cl, and Cl···Cl "bonds" were constrained with SHAKE, using a time step of 1 fs. A residue based cutoff of 12 Å was used for the nonbonded interactions.

The biphasic solvent system was built from two adjacent "rectangular" boxes of pure chloroform and water (Figure 2). The number of solvent molecules and the sizes of the cells are presented in Table 1. The concentration of the solutes, relative to the whole liquid system, is about 0.05 mol/L.

The MD simulations were performed in the (*N,V,T*) ensemble using a density rescaling procedure before minimization in order to start with the experimental density of chloroform (1.49 g cm^{-3}).[45] MD simulations were started with random velocities at 300 K, and the temperature was controlled by coupling to a thermal bath[46] with a relaxation time of 0.2 ps.

In principle, it would be desirable to use periodic boundary conditions along the three directions, as we did for the free MD simulations.[31,32] However we found that when this procedure was applied for the PMF calculations, the interface was moving with some solutes, as a result of their strong attraction. To avoid this artifact, we decided to apply the periodic boundary conditions along the *x, y* directions only (Figure 2). The solvent atoms close to the z_{water} and z_{chloro} boundaries were prevented from evaporation via a restraining potential of $k(z - z_{\text{water}})^2$ and of $k(z - z_{\text{chloro}})^2$ for the water and the chloroform molecules outside the box, respectively, with $k = 10$ kcal/mol Å.[2]

PMF Calculations. We defined two dummy atoms DU1 and DU2 at fixed positions (Figure 2) having the same *x, y* coordinates as the atom A of the solute. The PMF was obtained by moving step by step the *z* coordinate of A with respect to DU1 and DU2, while the rest of the system was free to move. For the PMF calculation of Cs^+ Pic^-, Cs^+ Cl^-, LCs^+, and LCs^+ Pic^-, A was Cs^+. Thus, no constraint was imposed on the ligand L or to the counterions. For L uncomplexed, a carbon atom of the phenolic unit (noted hereafter **AI**) or of the crown ether chain (noted hereafter **AII**) were used as atom A (see Figure 1).

The PMF calculations of LCs^+ and LCs^+ Pic^- started with the structure of the solute obtained after 350 ps of free MD simulation,[32] placed at the interface with Cs^+ slightly on the water side (Figures 5 and 6). For the L free run, we started with the geometry and position of LCs^+, where Cs^+ was removed (Figure 4). These systems were first equilibrated for 25 ps, with a position constraint on all the atoms of the solute.

For the PMFs of Cs^+ Pic^- and Cs^+ Cl^- salts we built the starting configurations in two steps, to start with Cs^+ at the interface. The ion pairs were first fixed on the water side of the interface and the solvents equilibrated for 25 ps. Then, for another 10 ps, only Cs^+ was fixed while Pic^- and Cl^- were free to move. Indeed, it was not possible to start from a free MD simulation because Cs^+ spontaneously migrates to water, as does Cl^-, while Pic^- remains adsorbed at the interface.

For each solute, two PMFs were calculated, where the A atom was moved step by step from the starting position at the interface ($d_{\text{chloro}} = d_{\text{water}} = 0$ Å) into the chloroform phase ($d_{\text{chloro}} = 10$ Å) and into the water phase ($d_{\text{water}} = 10$ Å), respectively (see Figure 2). For each PMF, the *z* position of A was increased from $d_1 = 0$ (starting position: $\lambda = 1$) to $d_0 = 10$ Å (final position: $\lambda = 0$), considering $d_\lambda = \lambda d_1 + (1 - \lambda)d_0$. The space between d_1 and d_0 was divided into 200 "windows", corresponding to an increment Δd of 0.05 Å ($\Delta\lambda = 0.005$). At each window, the difference in free energy between the states λ and $\lambda + \Delta\lambda$ ("forward calculation") and between the states λ and $\lambda - \Delta\lambda$ ("backward calculation") was calculated by

$$\Delta G_{\lambda_i} = G_{\lambda_{i+1}} - G_{\lambda_i} = -RT \ln\left\langle \exp - \frac{U\lambda_{i+1} - U\lambda_i}{RT} \right\rangle_{\lambda_i}$$

where R is the molar gas constant and T is the absolute temperature. $\langle\,\rangle\lambda_i$ stands for the ensemble average at the state λ_i where U_{λ_i} is the potential energy. At each window, 0.5 ps of equilibration were followed by 1.5 ps of MD for data collection and averaging for all systems. The only exception concerns the LCs^+ Pic^- complex where 2.5 ps were used for data collection in the "standard" calculations. In addition, for this system, two additional longer simulations were performed for comparison. The first one uses the same conditions, but a 12−18 Å twin cutoff, instead of a 12 Å cutoff for the nonbonded

TABLE 1: Conditions of Simulation: Number of Solvent Molecules, Box Size (Å³)

	free ligand L	LCs^+	$LCs^+ Pic^-$	$Cs^+ Pic^-$	$Cs^+ Cl^-$
nb chloro	501	430	501	336	213
nb water	1403	1515	1547	1143	1136
box size	36 × 37 × 110	35 × 37 × 106	41 × 35 × 105	35 × 28 × 105	27 × 29 × 105

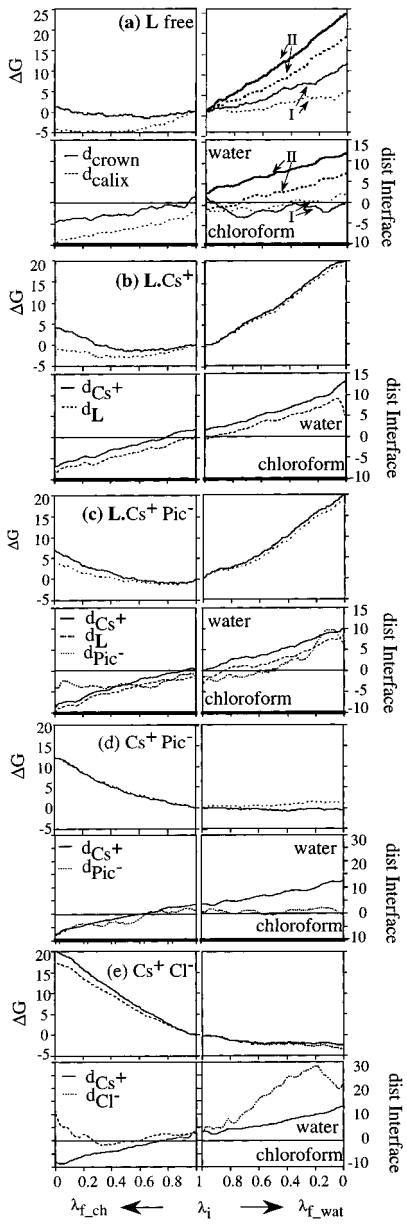

Figure 3. (a) PMF results for L free, (b) LCs^+, (c) LCs^+ Pic^-, (d) Cs^+ Pic^-, (e) Cs^+ Cl^-. For each system, the upper curve represents the free energy difference ΔG (kcal/mol) as the A atom is moved from the interface to chloroform (left-hand side) and to water (right-hand side). The full and dotted lines correspond respectively to the forward and backward cumulated free energies. The lower curve represents the distance from the interface to the center of mass of L, Pic^-, Cs^+ (Å). For L free the A atom (**AI** or **AII**) is defined in Figure 1. The position of the interface is recalculated at each step (see text).

interactions. The second one uses a 12 Å cutoff, but enhanced sampling (2.5 + 5 ps) at each window (i.e., every 0.05 Å of the "reaction coordinate").

Analysis of Results. The trajectories were saved every 2 ps, and their analysis was performed with the MDS[47] and DRAW[48] software. The *z* position of the interface (Gibbs dividing surface[10]) was defined as the intersection of the density curves of the two liquids which was recalculated every step. The position of the different moieties of the solute (the whole ligand L, its crown ether and its phenolic units, the Pic^- counterion, and the Cs^+ and Cl^- ions) with respect to the interface was defined by the *z* distance between their center of mass and the interface. The distance curves are presented in Figure 3 below the corresponding ΔG's. Schematically, L has a C_2 symmetry axis passing through the center of mass of the crown and of the phenolic rings. This axis is used to define the orientation of L with respect to the interface.

The interaction energies between different groups (water, chloroform, cation, anion, and ligand) have been recalculated from the trajectories along the PMF and are presented in Figure 9.

Results

In the following, we describe the general features of the PMF's which were obtained in the same conditions and the structural events that occur as the A atom (Cs^+ in all cases; excepted for L free) is moved from the interface to chloroform and to water, respectively, as well as the corresponding average interaction energies between the solute and the solvents. The free energy profiles and distances to the interface are shown Figure 3. Typical structures at the beginning of the PMFs, at the free energy minimum and at final positions in water and in chloroform, are shown Figures 4−8. The simulations on LCs^+ Pic^- with the larger cutoff and with enhanced sampling are considered in the discussion section.

1. Uncomplexed Ionophore L. The free energy profile for L (Figure 3a) displays a shallow miminum close to the interface on the chloroform side, and a steep increase on the water side (of about 20 kcal/mol, relative to the minimum).

Migration into Chloroform. At the beginning of the PMF simulation, the crown ether of L is on the water side while the aromatic groups are on the chloroform side of the interface (Figure 4). At the end, the latter are surrounded by chloroform, while the crown moiety remains in contact with the water phase via water molecules which form a hydrogen-bonded relay with one water molecule "complexed" by L, as was observed after 350 ps of free MD simulation.[31,32] Upon migration of L from the interface into chloroform, its increased interaction energy with chloroform (from −40 to −50 kcal/mol) compensates for the decrease in interaction with water (from −50 to −40 kcal/mol) (Figure 9).

Migration into water. L displays a marked reluctance to move into water. Indeed, when one of its aromatic carbon atoms (**AI** atom) is used to drive the PMF, L is "pushed " to water, but does not go there. It rotates and remains close and parallel to the interface. This is why we recalculated a second PMF where the crown was forced to move more deeply in water. For this purpose we chose as atom A the central carbon of the crown (labeled **AII**). Indeed, at the end of the **AII** PMF, the more lipophilic crown ether moiety is completely in water, while the aromatic groups are on the water side of the interface, still in contact with chloroform molecules. In the **AI** and **AII** PMFs, the free energy increases, but more with **AII** than with **AI** (21 and 8 kcal/mol, respectively), due to the deeper positioning of L in water (Figures 3a and 4). However, the final hydration scheme of L is identical in the **AI** and **AII** simulations: one "complexed" water molecule bridges over two phenolic oxygens

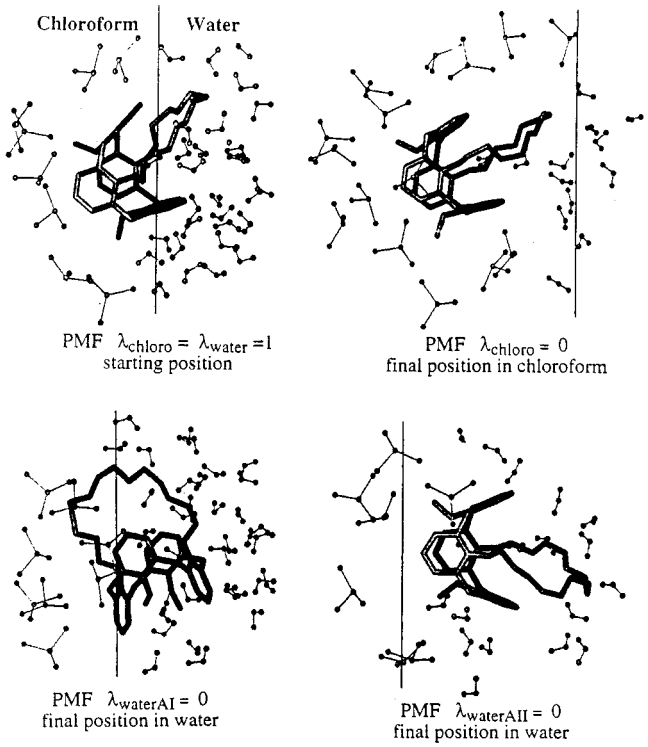

Figure 4. Typical structures taken along the PMF calculations of L, with selected solvent molecules. The vertical line delineates the (recalculated) position of the interface.

and is hydrogen-bonded to the bulk water via another water molecule (Figure 4).

It is noticeable that the large increase in free energy as L is moved into water is not due to a change in solute−solvent interactions (Figure 9). Indeed, although L is not soluble in water, its interaction energy with water (E_{L_water}) becomes more attractive and compensates more or less for the loss of interactions with chloroform (E_{L_chloro}). The changes are, as expected, largest in the **AII** PMF, where E_{L_water} changes from −50 to −70 kcal/mol, while E_{L_chloro} drops from −40 to −20 kcal/mol. The latter value is nonzero because L is in contact with chloroform.

2. LCs^+ Complex. Figure 3b shows that the free energy profile of the complexed ionophore is qualitatively similar to that of the uncomplexed one. The profile raises markedly on the water side of the interface (by about 20 kcal/mol) and displays a shallow mimimum on the chloroform side, somewhat more pronounced than with L, at a Cs^+ − interface distance of about 2.5 Å ($\lambda_{chloro} \approx 0.5$). This mimimum corresponds to about −1.7 kcal/mol of stabilization, compared to the final position in chloroform.

Migration into Chloroform. At the beginning of the simulation, LCs^+ sits at the interface with Cs^+ and the crown ether moiety situated on the water side, while the aromatic groups are on the chloroform side (Figure 5). At the free energy minimum (Figure 5), the position of Cs^+ with respect to the interface is essentially identical with that of the free MD simulation (the average distance Cs^+ − interface was 2.48 Å[32]). Until the end of this PMF calculation, one water molecule remains coordinated to Cs^+ and bridged to the interface by 4 to 5 water molecules (Figure 5).

Upon migration of LCs^+, the Cs^+−chloroform, Cs^+−L, and L−water interaction energies do not change significantly (Figure 9b). However, the $E_{Cs^+-water}$ attraction decreases from −60 to −35 kcal/mol, while the $E_{L-chloro}$ attraction increases only

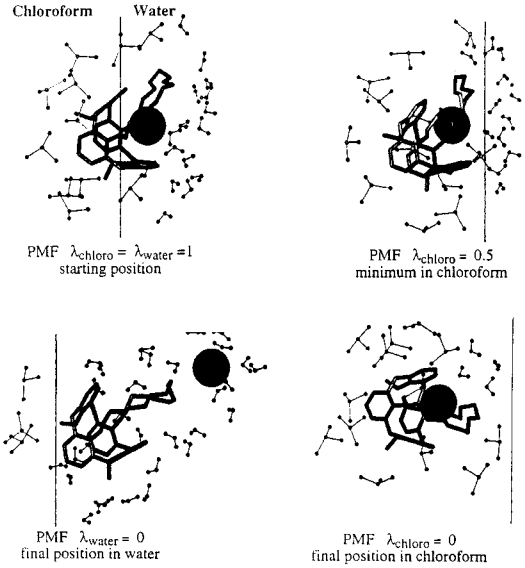

Figure 5. Typical structures taken along the PMF calculations of LCs^+, with selected solvent molecules. The vertical line delineates the (recalculated) position of the interface.

from −40 to −55 kcal/mol. This may explain why LCs^+, which is somewhat more hydrophilic than L alone, displays a more pronounced free energy minimum on the chloroform side of the interface.

Migration into Water. From the beginning of the simulation until nearly the end, Cs^+ which is moved into water, remains surrounded by the ligand L and the LCs^+ complex is of the inclusive type. However, at the penultimate point of the PMF ($\lambda_{water} = 0.1$), Cs^+ suddenly decomplexes while L returns to the interface (Figures 3b and 5). This is why the increase in free energy for LCs^+ is close to the one calculated for L uncomplexed. Interestingly, such a decomplexation of Cs^+ was not observed in the bulk liquid chloroform or aqueous phases.[32] It results from the asymmetrical environment of the complex at the interface, from the high affinity of L for the interface, and from the large increase of the $E_{Cs^+-water}$ attraction energy (from −50 to −120 kcal/mol) upon decomplexation (Figure 9b). As L, after decomplexation, returns to the interface, its final interaction energy with water is quite large (−70 kcal/mol, which is 83% of the interaction energy calculated from a bulk water simulation[31]). A significant contribution comes from a few water molecules "complexed" by L and from others which form a relay between L and Cs^+ (Figure 5). At the end of this simulation, the Cs^+ position is constrained, but after a few picoseconds of free MD, Cs^+ migrates to the bulk aqueous phase, while L remains at the interface.

3. LCs^+Pic^- Complex. The Pic^- counterion has no marked effect on the free energy profile of the LCs^+ complex (Figure 3c): ΔG rises steeply on the water side (by about 20 kcal/mol) and displays a minimum on the chloroform side, more pronounced, however, than that in the absence of the Pic^- anion ($\Delta G = -5.5$ kcal/mol, relative to the final state in chloroform). At the free energy minimum ($\lambda_{chloro} = 0.835$), Cs^+ sits at the interface, at a distance of 0.5 Å, close to the average distance of 0.8 Å found after a free MD simulation.[31,32]

Migration into Chloroform. At the end of this PMF simulation, the complex is situated in chloroform, with 5 or 6 water molecules building a bridge between Cs^+ and the water phase. The Pic^- counterion remains in close contact with the interface (Figure 6), separated from Cs^+ by a water molecule. Pic^- displays larger attractions with water than with chloroform (−60

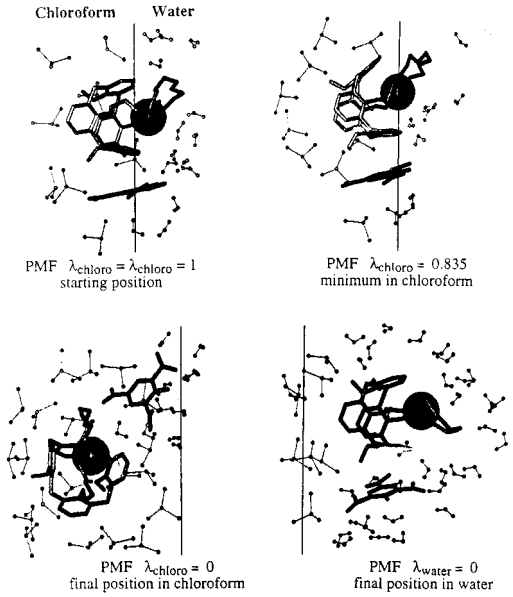

Figure 6. Typical structures taken along the PMF calculations of LCs^+ Pic^-, with selected solvent molecules. The vertical line delineates the (recalculated) position of the interface.

and −40 kcal/mol, respectively). The interaction energies Cs^+-solvent, Cs^+-L, and L-solvent are comparable to those calculated for LCs^+.

Migration into Water. As Cs^+ is moved into water, it remains complexed by L (Figure 6), in contrast to the decomplexation which took place in the absence of counterion. This is presumably because Pic^- stacks over a phenolic group of L, as in bulk water,[31] and attracts Cs^+ inside the host (by about −40 kcal/mol). The interaction energies change markedly when Pic^- has left the interface (at $\lambda_{water} = 0.3$, corresponding to a Cs^+-interface distance of ≈7 Å and to a Pic^-−interface distance of ≈2 Å). The Pic^-−chloroform interaction drops to zero, while the Pic^-−water attraction increases to −80 kcal/mol. At the end of this PMF, L sits in the water phase, perpendicular to the interface, accompanied by the anion (Figure 6).

4. Cs^+ Pic^- and Cs^+ Cl^- Salts (Uncomplexed). As expected, these two salts display a contrasting behaviors, when compared to the free or complexed calixarene (Figure 3d,e). Their migration from the interface to water corresponds to a slightly downhill energy process, while migration to chloroform is a high-energy process (by about 12 and 19 kcal/mol, respectively), with no free energy minimum. In addition, comparison of the two PMF's shows that the energy cost for "pushing" Cs^+ into the organic phase is lower with the Pic^- than with the Cl^- counterion, in relation to the differences on interfacial activities (see below for more discussion on this topic). Typical structures are shown in Figure 7 (Cs^+ Pic^-) and Figure 8 (Cs^+ Cl^-).

Migration of Cs^+ into Chloroform. The Pic^- and Cl^- counterions, which are free of constraints, behave differently, when Cs^+ is moved into bulk chloroform. The more "lipophilic" Pic^- anion follows Cs^+, up to a final distance of 7 Å from the interface (Figures 3d and 7). This contrasts with the hydrophilic Cl^- anion which initially follows Cs^+ as an intimate ion pair (until $\lambda_{chloro} = 0.25$; $d_{Cs^+_{interface}} = 2.5$ Å), but then suddenly dissociates and diffuses back to the water phase (Figure 8). Further details are given below.

In the Cs^+ Pic^- PMF, Pic^- sits initially in the plane of the interface, while Cs^+ is slightly on the water side and surrounded by water molecules (Figure 7). The ions are about 8.7 Å apart,

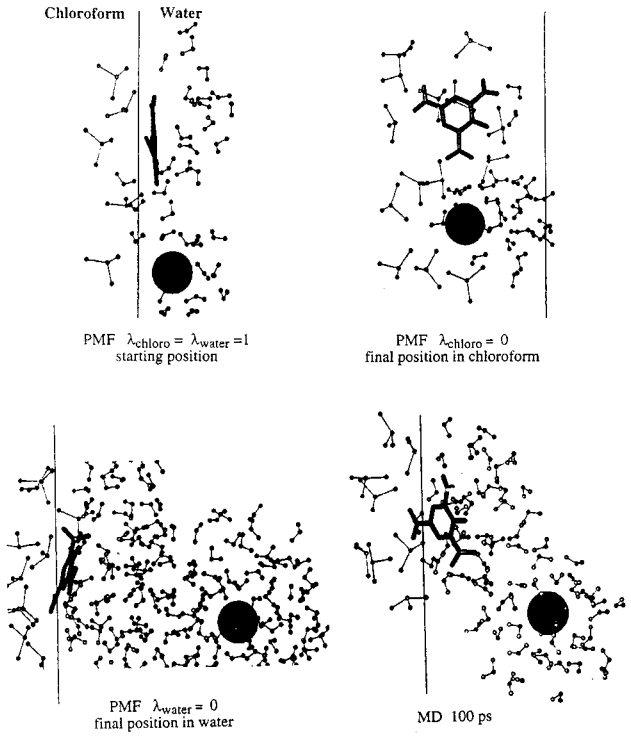

Figure 7. Typical structures taken along the PMF calculations of Cs^+ Pic^-, with selected solvent molecules. The vertical line delineates the (recalculated) position of the interface.

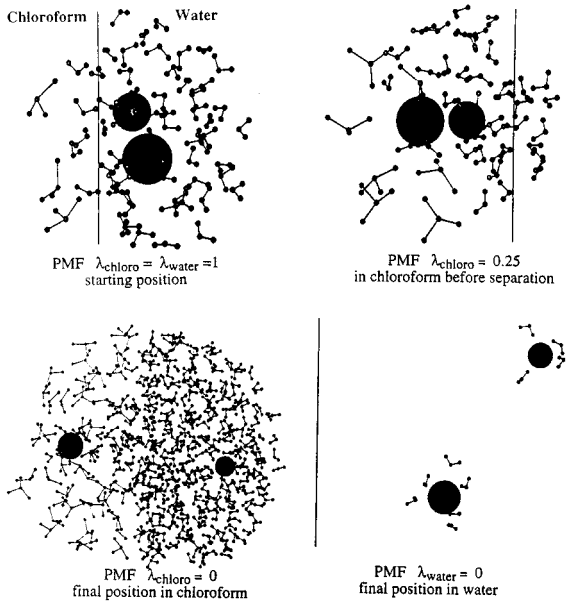

Figure 8. Typical structures taken along the PMF calculations of Cs^+ Cl^-, with selected solvent molecules. The vertical line delineates the (recalculated) position of the interface.

separated by water molecules, and attract each other by −40 kcal/mol (Figure 9d). As Cs^+ is moved by 10 Å into chloroform, it retains part of its hydration shell (five water molecules), linked to the water phase by a "water cone" of about 10 water molecules (Figure 7). This is why $E_{Cs^+-water}$ drops only from −100 to −80 kcal/mol. The Pic^- counterion follows Cs^+, separated by a few water molecules, and becomes perpendicular to the interface, pointing its O^- oxygen toward water. At the end of this simulation, it has lost about 40 kcal/mol of interaction energy with water (from −80 to −40 kcal/mol), and gained about 20 kcal/mol from interactions with chloroform (from −20 to −40 kcal/mol).

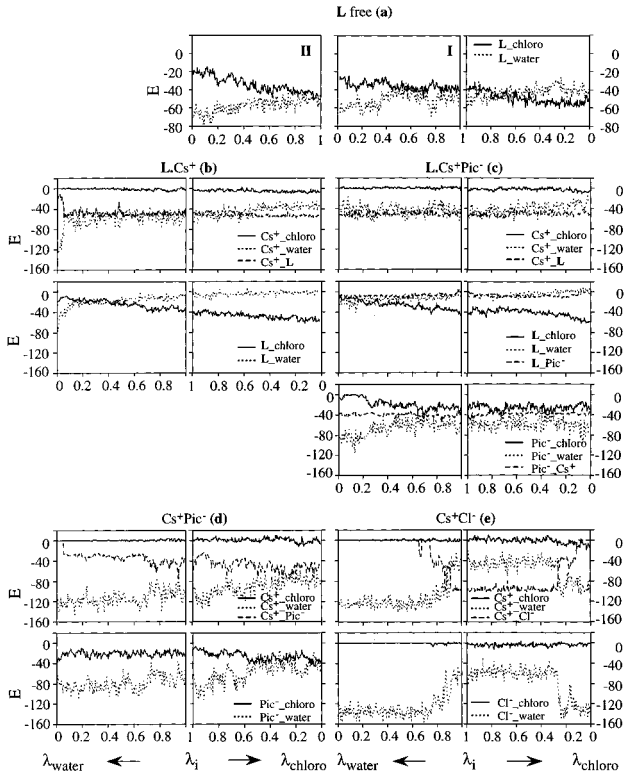

Figure 9. Average interaction energies (kcal/mol) calculated along the PMFs, as a function of λ (initial state at the interface, $\lambda = 1$; final state in chloroform, $\lambda_{chloro} = 0$; final state in water: $\lambda_{water} = 0$). Interaction between Cs^+, the counterion L, and the two solvents for (a) L free, (b) LCs^+, (c) LCs^+ Pic^-, (d) Cs^+ Pic^-, (e) Cs^+ Cl^-.

The Cs^+ Cl^- PMF simulation to chloroform corresponds to a different situation. At the beginning, the two ions are in contact and Cl^- is at the interface (Figure 8). They are surrounded by 12−15 water molecules, and strongly attract each other (−90 kcal/mol). As Cs^+ is moved into chloroform, the ion pair dissociates and Cl^- returns into water, due to the strong increase in its hydration energy (from −40 to −130 kcal/mol). Until the end of this simulation, Cs^+ remains connected to the interface by a "water cone" (Figure 8), similar to that observed for Cs^+ Pic^- . As a result, the "hydration energy" of Cs^+ reaches the same value of −80 kcal/mol, as the one calculated with Cs^+ Pic^-.

Migration into Water. When Cs^+ is moved to the water side of the interface, both counterions dissociate from Cs^+, but Pic^- remains "adsorbed" at the interface, while Cl^- diffuses rapidly to the bulk water phase. In the two cases, the free energy profiles are rather flat, but for Cs^+ Cl^- the energy decreases to a lower value (−2.5 kcal/mol) than for Cs^+ Pic^-.

With the two counterions, Cs^+ ends up with similar interaction energies with water (−120 kcal/mol) and has no interaction with chloroform.

Discussion

On the basis of computer MD-FEP simulations starting at the water−chloroform interface, we compare the energetics of the first stages of migration to the chloroform and to the water phases, respectively, for a free and complexed ionophore, and for two uncomplexed salts. Before discussing the results further, it is important to note that, due to computer limitations, a short distance (10 Å) on each side of the interface was investigated. Thus, the change in ΔG's, as the cation or the ligand are moved 10 Å away from the interface may contribute a small part of the complete energy profile for crossing the interface. Despite these limitations, a number of different behaviors were observed. For the free salts, diffusion from the water phase to the interface corresponds to a modest energy cost (a few kcal/mol), which is lower with the Pic^- anion than with the Cl^- anion. However, the migration of the free cation to the organic phase is a high energy process. This contrasts with the ligand L, free or complexed, which would be "expelled" by water and adsorbed at the interface on the chloroform side. Other important features revealed by our study concern the role of counterions in ionophore assisted interface crossing: the Pic^- anion is highly surface active, while Cl^- is not. These results, based on the computations, are fully consistent with related experimental data and have important implications concerning the assisted ion transfer and interfacial electrochemistry. They are discussed below.

1. Why Do the Free and Complexed Ionophore Adsorb at the Interface? Energy Component Analysis and Comparison with Experimental Data. For the free ionophore, as well as for its complex, we calculate a free energy minimum near the interface on the chloroform side. This may seem in contradiction with the fact that L and related calixarene ionophores are good extractants for alkali cations, and particularly for Cs^+.[37,49]

TABLE 2: Solute (S) at the Chloroform−Water Interface and in Bulk Solvents[a]

	interface			pure solvents	
	$E_{S\cdots chloro}$	$E_{S\cdots water}$	$E_{S\cdots solvent}$	$E_{S\cdots chloro}$	$E_{S\cdots water}$[b]
free ligand L	−37	−33	−70	−68	−84, 83%
LCs^+	−45	−43	−88	−77	−106, 83%
LCs^+ Pic^-	−60	−92	−152	−100	−177, 86%

[a] Average interaction energies (kcal/mol) for solute−chloroform ($E_{S\cdots chloro}$) and solute−water ($E_{S\cdots water}$) after free MD simulations at the interface and in bulk solvents.[32] $E_{S\cdots solvent} = E_{S\cdots chloro} + E_{S\cdots water}$ at the interface. [b] Interaction with the two solvents at the interface, relative to the interaction with bulk water (%).

The reluctance of L, LCs^+, and LCs^+ Pic^- to diffuse from the interface into water cannot be explained by the solute−solvent interactions. The energy component analysis performed near the free energy minimum shows that, although these species are on the chloroform side of the interface, they are attracted by water to a similar extent, or even more than by chloroform. As, at the interface, their total interaction energies with the two solvents is smaller than the interaction observed with a bulk water simulation (Table 2), migration to water would enhance their "solvation energies". Such migration does not occur however because of the solvent−solvent cohesive forces. As water has a surface tension much larger than chloroform (72.9 and 26.7 mN/m, respectively)[10] the "cavitation energy" (energy cost for creating a cavity) is much larger in water than in chloroform.[50] On the other hand, these solutes do not interact enough with water to compensate for this cavitation energy.

Now comes the question of why L, LCs^+, and LCs^+ Pic^- do not spontaneously migrate to the organic phase. As these solutes move further into chloroform, the free energy increases, but much less than it does in the water phase, first because the cost of creating a cavity is less. Second, water molecules follow the solutes from the interface to the chloroform phase, whereas no chloroform molecules follow the solute to the water side. At the interface, the most hydrophobic L or LCs^+ solutes interact to a similar extent with chloroform and the water phases, but LCs^+ Pic^-, which is somewhat more hydrophilic, has larger interactions with water (Table 2). As a result, the distance

between the cation and the interface at the minimum is smaller for LCs^+ Pic^- (0.5 Å) than for LCs^+ without counterion (2.5 Å). *Thus, the free and complexed ionophores adsorb at the interface because of their strong hydrogen bonding connections to the bulk water phase and of the lower surface tension of the organic liquid.*

Our findings are consistent with experimental results on related extractant systems. The Gibbs adsorption theorem[10] relates the surface tension σ to the (algebraic) excess of interfacial concentration of the solute relative to that in the bulk c_{bulk}. Surface tension measurements with solutions of extractant molecules, like alkylphosphoric acids and esters,[51] ethers, crown ethers, show that σ decreases as c_{bulk} is increased, as observed for surfactants.[52] Thus their concentration at the surface should be larger than in the bulk organic phase. For tri-*n*-butyl phosphate (TBP) it was estimated that the enthalpy of adsorption at a *n*-dodecane-water interface is comparable to, or somewhat larger than the enthalpy of transfer from water to *n*-dodecane (about −10.9 and −10.3 kcal/mol, respectively).[53] These energies are somewhat more negative than for typical amphiphilic molecules such as *n*-octanol (−7.4 and −6.2 kcal/mol, respectively). TBP complexes of $Cu(NO_3)_2$ or $Li(NO_3)$ are more surface active than the free TBP.[54] In another study, Danesi et al.[55] investigated the transfer rate of K^+ ions from water to 1,2 dichloroethane containing dibenzo-18-crown-6 (DBC). On the basis of interfacial tension measurements at the water−benzene interface they concluded that DBC forms an adsorbed layer at the interface, when the DBC concentration reaches 0.5×10^{-3} mol/L. When DBC is dissolved in benzene and the inorganic salt MX is present in the aqueous phase, DBC·MX complexes are formed at the interface, where they display higher surface activity than DBC.[56] In the case of cation-exchange extractants such as alkylphosphoric acids, the better extractable cations promote the adsorption of the extractant at the interface between air and water solutions of inorganic salts.[57] These results are fully consistent with the more pronounced minimum we calculate for L complexed, compared to L free. At the air−water interface, which displays obvious analogies with the chloroform−water interface, ionophores such as calixarenes,[58] crown ethers,[59] and their lipophilic derivatives[60] form monolayers, as does phenol itself,[25,61] a basic component of calixarenes. Despite their mutual electrostatic repulsions, bicylic [222] Na^+ cryptates form a monolayer at the water−mercury interface, on the side of the liquid with lowest surface tension.[62] Kinetic studies on transport with DBC at an aqueous−chloroform interface led to the assumption that the interface consists of a fully condensed monolayer of the ligand.[63] Other examples can be found in refs 1, 5, and 9.

2. Facilitated Cation Transfer from the Interface to the Organic Phase upon Complexation. The comparison of the free energy curves for LCs^+ Pic^- and Cs^+ Pic^- (Figure 3c,d) shows that the complexation of Cs^+ by L facilitates the migration of the cation from the interface into chloroform. For instance a cation displacement of 7 Å from the interface to the chloroform phase increases the free energy by 5 kcal/mol for the complexed Cs^+, which is 7 kcal/mol less than that for the uncomplexed Cs^+. The energy component analysis for Cs^+/LCs^+ at this position shows dramatic differences. The uncomplexed Cs^+, surrounded by water molecules in the chloroform phase, is attracted by water (−80 kcal/mol) and does not interact with chloroform. The more lipophilic LCs^+ species is less attracted by water (−35 kcal/mol) but is more solvated by chloroform (−55 kcal/mol). This assisted transfer of the cation through the interface is consistent with the fact that in the water−chloroform extraction system, Cs^+ Pic^- is not transferred to the organic phases in the absence of extractant molecules, but is extracted by L.[37,49] Generally speaking, it is consistent with the extraction features of ionophores. Electrochemistry at ITIES on analogous systems[2,13] demonstrated the role of nonionic polyether surfactants[64] ionophores such as valinomycin, nonactin,[65] monensin,[66] crown ether derivatives[65,67] on the facilitated transfer of K^+, or of other cations. Our results and these experimental data indicate that *assisted ion transfer corresponds also to a high interfacial activity of the complexed ion.*

3. Interfacial Role of the Anion. Our simulations on LCs^+ Pic^- and on Cs^+ Pic^- demonstrate the high affinity of Pic^- for the interface, while Cl^- is captured by water and fully dissociated from the free or complexed cation. As a result, the free energy increase upon migration of Cs^+ uncomplexed from the interface into chloroform is weaker with the Pic^- than with the Cl^- counterion (12 and 19 kcal/mol, respectively, at the end of the PMF). Such counterion effect is fully consistent with related experimental results on extraction systems. For instance, the surface activity of DBC·MX complexes at the benzene-water interface is considerably affected by the X^- anion of the metal salt, and increases with the decreased hydration energy of X^- ($F^- < Cl^- < NCS^- < ClO_4^-$ for $M^+ = Na^+$), and with the stability of the DBC·MX complex ($Na^+ < K^+$).[56] Similar effects were observed when the transfer kinetics of MX salts across the liquid membranes containing DBC was studied.[68] Another example concerns the extraction rate of Fe^{2+} by 1,10-phenanthroline ligands, which was ascribed to the interfacial adsorptivity of the complexes in accordance with the sequence of the hydration energy of the X^- counter ion[7] ($ClO_4^- < CCl_3COO^- < Br^- < Cl^- < SO_4^{2-}$). The Pic^- ion, not reported in that series, should be on the left-hand side, as it is more easily transferred from water to organic solvents than ClO_4^- (the difference in the free energies of transfer amounts to about 1.8 kcal/mol for 1,2-dichloroethane or nitrobenzene as organic solvents[69]). Our results and these experimental data point out another important feature, related to the interfacial activity and concentration of X^-, which may critically determine the rate of extraction; *the anions adsorbed at the interface attract the cations from the aqueous phase to the interface, where the formation of the complex is facilitated.*

Another facet concerns electrochemistry. For the uncomplexed Cs^+ Pic^- salt, adorption of Pic^- at the interface leads to a charge separation, with a negatively charged interface and a positively charged inner aqueous solution (Cs^+). The interfacial electrochemical potential should be therefore more negative with Cs^+ Pic^- than with a Cs^+ Cl^- salt, where the interface should be free of ions. For the complexed state of the cation, we simulated Pic^- only as counterion, as it is clear that more hydrophilic anions such as Cl^- will migrate to the aqueous phase, while the interface, covered by the cation complexes, is positively charged. Thus, the interfacial potential should be smaller with Pic^- than with Cl^- as counterion. To our knowledge, these potentials have not been measured for cation complexes as a function of the counterion. However, for aqueous electrolyte solutions of monoatomic cations with different anions, surface potential measurements lead to a negative potential, resulting from a closer proximity of the anions to the interface, compared to the cations.[70,71] If the anions are arranged in order of increasing surface potentials for solutions of their salts, one obtains the lyotropic series[70] also known as the Hofmeister series,[72] which follows the sequence of their decreasing hydration energies, and their propensity to

adsorb at the water−organic liquid interface:

$$SO_4^{2-} < F^- < Cl^- < Br^- < NO_3^- < I^- < ClO_4^- < SCN^- < PF_6^-$$

Although no values have been reported to our knowledge for Pic^-, this anion should be found on the right-hand side of the series and display a high affinity for the interface. This contrasts with electrolytes which have only a small effect on the surface potential of water (e.g., alkali chlorides[73]) where cations and anions are thought to be "repelled" from the surface, leaving a solute free layer 4−5 Å thick.[2,13]

On the computational side, Benjamin[29] compared the transfer of Cl^- from water to the water−vapor interface to the transfer of "Cl^+" (same Lennard-Jones parameters as Cl^-, but charge +1). They calculated that the cation experienced a somewhat larger resistance to being pushed to the interface than the anion. Wilson et al.[24] investigated Na^+, F^- and Cl^- ions near the water liquid−vapor interface by MD simulations. While the anions can approach the interface up to two molecular layers without significant change in free energy, 2.5 kcal/mol are needed to move the cation the same distance. These differences are ascribed to the interaction of the ions with the water molecules in the interfacial region. Our calculated differences in Cl^-/Pic^- behavior at the interface are consistent with these theoretical and experimental results.

4. "Water Dragging Effect". At the final position of the PMF simulations into chloroform all systems are still in contact with the water phase via "water fingers" or a "water cone". For instance, three water molecules are directly coordinated to the free ligand L and establish a link to the water phase (Figure 4). About 4 or 5 water molecules bridge the complexed Cs^+ (LCs^+ and LCs^+ Pic^-) with the water phase (Figures 5 and 6). In those cases where the energy cost for moving to chloroform is lowest, the interface is relatively flat. This contrasts with the case of uncomplexed Cs^+, where the energy cost is highest, and the interface displays a water protuberance. Cs^+ retains its first hydration shell, connected by about 10−15 water molecules to the water phase (Figures 7 and 8). As the solutes were not pushed far enough into chloroform, it is not clear whether such water connections would be disrupted, or partly retained. However, even for the most hydrophobic L species, it is clear that the few firmly hydrogen bonded water molecules should remain as part of a "supermolecule" in the organic phase. As the total charge and amphiphilic character of the solute increase (upon cation complexation, or due to the counterion) more water should be dragged.

In ion extraction experiments, the water content of the organic phase is known to increase markedly. For instance, the hydration of crown ethers and their complexes has been measured in organic phases saturated with water.[5] For the systems we studied, that are however no such data. Generally speaking, systematic studies as a function of the ionophore and of the extracted ions are still lacking. Karl Fischer measurements of the excess water in organic solvents with polar organic solutes indicate that the hydrogen bond donating capacity of solutes plays a predominant role in the "water-dragging effect".[74] When more hydrophilic cationic species cross the interface, they should drag water as well. Previous computational studies of unassisted Cl^- transfer across a 1,2-dichloroethane-water interface[29] also showed the formation of "water fingers" connecting the ions with the interface, and the water leaking to the organic phase. The hydration we observe at the interface with neutral or charged solutes is qualitatively consistent with such data.

5. Computational and Experimental Aspects. In this section, we address some questions related to computational aspects and their relation with experiments. The first one concerns the physical representation of the system studied (size of the system, concentration in the bulk phases and at the interface, saturation, homogeneity, constraints, etc.). In practice, extraction experiments start by shaking the aqueous and organic phases, containing respectively the salts and the extractant molecules. In transport experiment, the liquid phases are agitated, leading presumably to the formation of "stagnant film" region.[1] In electrochemical studies of ITIES, an external constraint (electrical field) is imposed to the system. Thus, these situations may differ somewhat from the ones we simulated. Our deliberate choice was to select a similar starting state for all systems (solutes at the interface), and to test their response under well-defined constraints, identical for all of them. For some systems (those involving the L molecule), this closely corresponds to an equilibrium situation, and we explore the departure from the minimum. Other systems (e.g., free ion pairs) are far from an energy minimum, due to solvation effects and solvent cohesive forces. They are explored in a consistent way for all systems, which does not necessarily correspond to a full relaxation of the system. Full relaxation is prevented by constraints of the solvent molecules at the edges. For instance, when the free Cs^+ ion is moved in the direction of the organic phase, it is followed by the water phase, until some compression of the solvent phases is achieved. Another example concerns the Cl^- counterion which was initially constrained on purpose at the interface, because it otherwise complety migrates to water. The relaxation of the system depends thus on the constraints imposed to the solvent, as well as on the solute, and on the simulated time. Our approach is to compare the response of different systems, allowing a same relaxation (0.5 + 1.5 ps for most systems) at every window (i.e., after a small displacement (0.05 Å) of the moved atom A). The simulated time corresponds for the A atom to a displacement of 1 Å in 40 ps which, according to observations we made in free MD simulations on related systems is relatively "slow". For instance, when a similar salt was simulated in the same conditions, starting at 11 Å from the interface in the chloroform phase, it spontaneously moved back to "bulk water" in about 50 ps, (i.e., about 10 times faster that the rate of displacement imposed in our PMF simulations). During these 50 ps, the interface, initially flat, markedly first curved to the cation, to flatten again.[78] We reported another simulation where the LCs^+Pic^- solute, initially placed at 12 Å from the interface in chloroform, adsorbed in about 120 ps at the interface (see Figure 6 of ref. 32), as found here. We also performed a "demixion experiment", starting with an homogeneous binary water−chloroform solution of LCs^+Pic^-.[79] After 300 ps of free MD simulation, complete phase separation was achieved, the solute was adsorbed at the interface in a situation nearly identical with the one which corresponds to the free energy minimum of the PMF. Another demixion simulation, using a more polar model for chloroform (OPLS charges scaled by 3.0) led also to full demixion after 550 ps, with LCs^+Pic^- adsorbed at the interface.[79] Taken together, these results indicate that our sampling time at each window, used in conjunction with very small displacements, is reasonable.

In PMF calculations on ionic or molecular solutes at interfaces, Benjamin et al.[29] and Pohorille et al.[26] used another procedure, based on large windows (3 to 6 Å wide), and extensive sampling at each window (from 0.4 to 1 ns), where the solute was free to move in the three directions. This led us to test a new PMF simulation, based on a similar time scale.

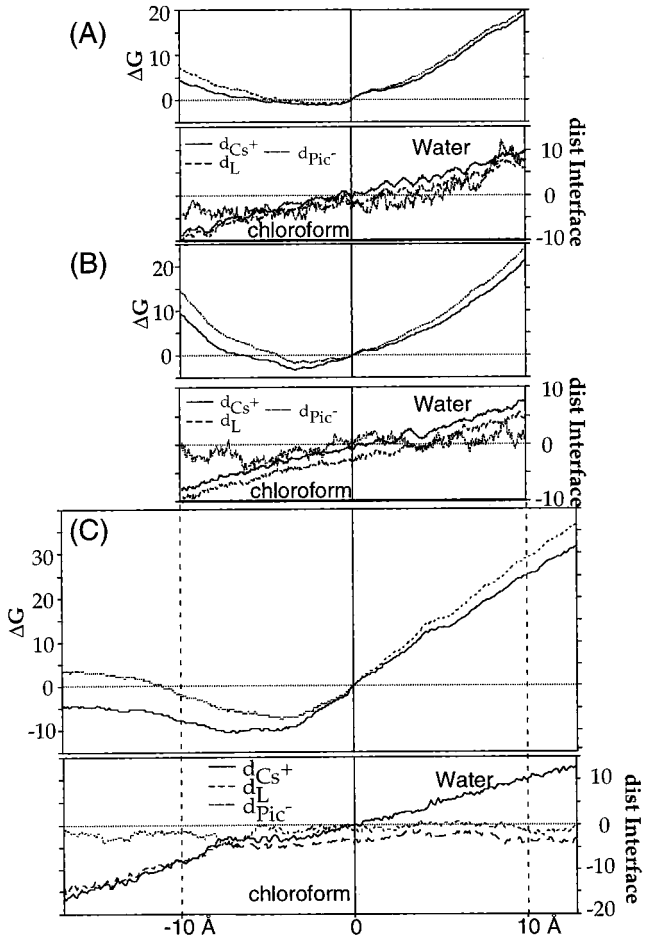

Figure 10. PMF results for LCs^+ Pic^- obtained by three different simulations. (A) Top: standard calculations (12 Å cutoff; 0.5 + 2.5 ps at each window), (B) middle: long-range nonbonded interactions (12−18 Å twin cutoff; 0.5 + 2.5 ps at each window), (C) bottom: enhanced sampling (12 Å cutoff, 2.5 + 5 ps at each window). For each system, the upper curve represents the free energy difference ΔG (kcal/mol) as the Cs^+ atom is moved from the interface to chloroform (left-hand side) and to water (right-hand side). The full/dotted lines correspond to the forward/backward cumulated free energies. The lower curves represent the distance from the interface to the center of mass of L, Pic^-, Cs^+ (Å). The position of the interface is recalculated at each step (see text). As the three simulations started with different configurations, a same origin has been defined for these curves. It corresponds to a zero Cs^+ distance to the (actual) interface. The *x* axis corresponds to the displacement of Cs^+ (in angstroms) along the PMF.

We chose the LCs^+Pic^- system, because of its crucial role in the assisted ion extraction process and because of its complexity (status of counterion, nature of the inclusive/noninclusive complex, position of the different moieties with respect to the interface). The PMF was recalculated in the same conditions are those reported above (cutoff of 12 Å, windows of 0.05 Å), but with enhanced sampling at the window (2.5 ps + 5 ps). Thus, 1 Å of Cs^+ displacement corresponds to 150 ps of simulation. The starting position was also somewhat different, as it resulted from a 300 ps of MD equilibration, where Cs^+ is not strictly "at the interface", but somewhat on the chloroform side. In addition, we explored a larger space at each side of the interface, spanning a total distance of 30 Å. The corresponding free energy curve is shown in Figure 10, together with the curve of Figure 3c, obtained with less sampling. For consistency, the origin of the abscissa has been chosen such that the Cs^+ position with respect to the position of the interface (recalculated at each window) is zero. Within the same range of distances from this origin, both curves are smilar and display a minimum on the chloroform side of the interface. Departure from this minimum is clearly more facile toward the organic, than toward the aqueous phase. The corresponding structures are also similar, and close to the ones found in the free MD simulations. In the PMF's to chloroform and to water, the Pic^- counterion does not follow Cs^+ and remains at the interface. In the standart calculation to water, Pic^- stacked over a phenolic ring of L. In fact, both arrangements are very likely. There are solid-state analogues of the Pic^- stacking, while there is strong evidence for adsorption of Pic^- at the interface.[56] With the enhanced sampling, migration to water leads to Cs^+ decomplexation, as described above for LCs^+. This confirms the low affinity of the complex and its counterion for the aqueous phase, compared to the interface. Concerning the left side of the PMF (migration to chloroform), there is now a plateau region, starting when Cs^+ is at more than 10 Å from the interface, (i.e., close to the cutoff distance). This plateau does not result therefore from enhanced sampling, but from the (arte)fact that the solute does not interact with water anymore. Thus, to conclude, enhanced sampling, although a priori more satisfactory, does not modify the conclusions based on shorter simulations.

For the other systems, it is likely that structural events that occur along the PMF depend on the sampling time. For instance, when Cs^+ Cl^- is moved to chloroform, the capture of Cl^- by water would certainly happen earlier in longer simulations, which contrasts with the behavior of Pic^-. It should be remembered however that such detailed structural events have no real physical meaning, as no Cs^+ transfer takes place spontaneously. On the other hand, in the presence of an electric field, Cs^+ and the anion would separate from each other.

Another important question concerns the role of long-range electrostatic interactions[77] on the interfacial behavior. This led us to simulate the LCs^+ Pic^- complex at the interface: (i) with a reaction field correction of the electrostatics beyond the 12 Å cutoff distance, (ii) with a 12 Å cutoff and the Ewald summation implemented in AMBER, and (iii) with a twin 12−18 Å twin cutoff distance.[78] In the three cases, after 300 ps of dynamics, the complex remained at the interface, in a position similar to that reported here for the free energy minimum. In addition, we recalculated the PMF of this complex in the same conditions are those reported in Figure 3, but using a 12−18 Å twin cutoff, instead of a 12 Å cutoff distance. The curve reported in Figure 10 shows that similar results are obtained with both cutoff distances. Migration from the interface to water leads to identical energy costs (20 kcal/mol at $\lambda_{wat} = 0$), while migration to chloroform is at higher energy with the 12−18 Å cutoff (by about 5 kcal/mol, for $\lambda_{chl} = 0$). Thus, the conclusion that the complex adsorbs at the interface is strengthened with the use of a larger cutoff. This result is easily understood by the fact that, at the interface, this amphiphilic solute "sees more water" and is more attracted with the 12−18 Å, than with the 12 Å cutoff. As far as the position of the solutes are concerned, it can be seen from Figure 10 that they are similar with the two cutoff distances.

At a more quantitative level, the results may depend on the empirical representation of the potentiel energy and the representation of solvents, whose parameters were derived from the pure liquid simulations. Polarization and many body effects of the solute and the solvents,[76] not included here, may also quantitatively modulate the energies. The dielectric constant of the solvents near the interface remains to be accounted for.[80] Other questions that we investigated by free MD simulations are the chloroform representation, the choice of (N,P,T)/(N,V,T)

thermodynamic ensembles,[32] the procedure of temperature monitoring.[78] In all cases, we observed a similar interfacial behavior for the LCs^+ Pic^- complex, which closely corresponds to the energy minimum reported here. All these results, and the agreement with all related experimental data thus suggest that despite the limitations pointed out above, the simulations correctly depict importance features in the interfacial behavior of ionophores, free and complexed, and of the accompanying counterions.

Conclusion

We presented free energy profiles for moving Cs^+ uncomplexed and complexed by a ionophore from a chloroform−water interface into the corresponding "bulk" solvents. The simulations confirm the high interfacial activity of L, LCs^+, LCs^+/Pic^- which display an energy minimum on the chloroform side of the interface at positions close to those obtained after free MD simulations of the three solute systems. *These amphiphilic species therefore behave like surfactants.* The facilitated ion crossing of the interface upon complexation is evidenced by the comparison of the free energy profiles of the uncomplexed Cs^+ Pic^- salt and of the LCs^+ Pic^- complex. As the energy profile beyond 10 Å from the interface has not been calculated with an adequate cutoff distance, we cannot conclude whether it remains more or less flat, or decreases to a more stable state (i.e., whether the interface corresponds to an absolute or to a local energy minimum).

Based on the calculated surfactant behavior of the free and complexed ligand, it can be speculated that the assisted cation extraction mechanism involves adsorption of the ligand and of the anion at the interface, a series of complexation equilibria, and desorption of the adsorbed complex into the organic phase.[5,7,9] Desorption may be facilitated by an increased interfacial concentration of the complex, of the extractant molecules, counterions, as well as of surfactants which reduce the interfacial pressure. A significant part of the synergistic effects brought about by other cation-binding molecules may result from their adsorption at the interface.[75,81]

Our study calls for experiments and theoretical investigations on the interfacial behavior of calixarenes and related ionophores. We focused on the Cs^+ complex (i.e., on the cation which is selectively complexed by L among other ions present in nuclear waste disposals[37,49]). The question of ion recognition has to be investigated at the interface.[82] With increased computer resources, further insights will be obtained on what happens away from the interface, at distances larger than the one investigated here. Consistent comparisons with other systems involving cations and counterions of different charge and lipophilicity, solvents, ionophores will provide energy and related structural features, leading to a better understanding of the selective processes. What happens with ions at the water−liquid interface has a bearing on recognition and extraction chemistry, phase transfer catalysis, electrochemistry, as well as on the specific interactions that occur at the surface of organized systems such as micelles, microemulsions and lamellar phases[83] or of ion-crossing through membranes.[84]

Acknowledgment. The authors are grateful to CNRS and IDRIS for allocation of computer resources, to PRACTIS for support, and to Prof. K. Merz for helpful discussions. Grants from the French Ministery of Research (for ML and NM) and EEC (F14W-CT96-0022 for LT) are also acknowledged.

References and Notes

(1) Danesi, P. R. In *Principles and Practices of Solvent Extraction*; Rydberg, J.; Musikas, C. Chopin, G. R., Eds.; M. Dekker, Inc.: New York, 1992; pp 157−207.

(2) Girault, H. H.; Schiffrin, D. J. In *Electroanalytical Chemistry*; Bard, A. J., Ed.; Dekker: New York, 1989; pp 1−141.

(3) *The Interface Structure and Electrochemical Processes at the Boundary between two Immiscible Liquids*; Kazarinov, V. E. Ed.; Springer: Berlin, 1987.

(4) Marcus, Y.; Kertes, A. S. *Ion Exchange and Solvent Extraction of Metal Complexes*; Wiley-Interscience: New York, 1969.

(5) Moyer, B. A. Molecular Recognition: Receptors for Cationic Guests, In *Comprehensive Supramolecular Chemistry*; Atwood, J. L., Davies, J. E. D., McNicol, D. D., Vögtle, F. Lehn, J.-M., Eds.; Pergamon: New York, 1996; Vol. 1, pp 325−365.

(6) Simon, W.; Morf, W. E.; Meier, P. C. *Struct. Bonding* **1973**, *16*, 113−160. Ovchinnikov, Y. A.; Ivanov, V. T.; Shkrob, A. M. *Membrane Active Complexones*; B. B. A. Library, Elsevier: Amsterdam, 1974. Ascher, P.; Gautheron, D.; Ptak, M.; Pullman, A.; Shechter, E.; Troyanovsky, C. *Physical Chemistry of Transmembrane Ion Motions;* Spach, G., Ed.; Elsevier: Amsterdam, 1983. Lehn, J. M. *Struct. Bonding* **1973**, *161*, 1−69. Dobler, M. *Ionophores and Their Structures*; Wiley-Interscience: New York, 1981. Lamb, J. D.; Izatt, R. M.; Christensen, J. J. In *Progress in Macrocylic Chemistry*; Izatt, R., Christensen, J. J., Eds.; Wiley: New York, 1981; p 42. Lehn, J. M. In *Physical Chemistry of Transmembrane Ion Motions*; Spach, G., Ed.; Elsevier: Amsterdam, 1983; pp 181−206. Lehn, J. M. *Angew. Chem., Int. Ed. Engl.* **1988**, *27*, 89−112. Lehn, J.-M. *Supramolecular Chemistry. Concepts and Perspectives*; VCH: Weinheim, New York, 1995. Behr, J. P.; Kirch, M.; Lehn, J. M. *J. Am. Chem. Soc.* **1985**, *107*, 241−246. Visser, H. C.; Reinhoudt, D. N.; de Jong, F. *Chem. Soc. Rev.* **1994**, 75−81.

(7) Watarai, H. *Trends Anal. Chem.* **1993**, *12*, 313−318.

(8) Starks, C. M.; Liotta, C. L.; Halpern, M. *Phase Transfer Catalysis*; Starks, C. M., Ed.; Chapmann and Hall: New York, 1994. Lasek, W.; Makosza, W. *J. Phys. Org. Chem.* **1993**, *6*, 412−420. Dehmlow, E. V.; Dehmlow, S. S. *Phase Transfer Catalysis*; Verlag Chemie: Weinheim, 1983. Tan, S. N.; Dryfe, R. A.; Girault, H. H. *Helv. Chim. Acta* **1994**, *77*, 231−242.

(9) Danesi, P. R.; Chirizia, R.; Coleman, C. F. In *Critical Reviews in Analytical Chemistry*; Campbell, B., Ed.; CRC Press: Boca Raton, FL, 1980; pp 1−126.

(10) Adamson, A. W. *Physical Chemistry of Surfaces, 5th ed.*; Wiley: New York, 1990.

(11) Hiemenz, P. C. *Principles of Colloid and Surface Chemistry*; Lagowski, J. J., Ed.; M. Dekker, Inc.: New York, 1986.

(12) Koryta, J. *Ion Selective Electrode Rev.* **1983**, *5*, 131−164.

(13) Girault, H. H. *Electrochim. Acta* **1987**, *32*, 383−385.

(14) Vanysek, P. *Electrochim. Acta* **1995**, *40*, 2841−2847.

(15) Eisenthal, K. B. *Chem. Rev. (Washington, D.C.)* **1996**, *96*, 1343−1360. Shen, Y. R. *Annu. Rev. Phys. Chem.* **1989**, *40*, 327−50.

(16) Rice, S. A. *Nature* **1985**, *316*, 108. Pershan, P. S. *Faraday Discuss. Chem. Soc.* **1990**, *89*, 231−245.

(17) Wirth, M. J.; Burbage, J. D. *J. Phys. Chem.* **1992**, *96*, 9022−9025.

(18) Tohda, K.; Umezawa, Y.; Yoshigawa, S.; Hashimoto, S.; Kawasaki, M. *Anal. Chem.* **1995**, *67*, 570−577. Ding, Z.; Wellington, R. G.; Brevet, P. F.; Girault, H. H. *J. Phys. Chem.* **1996**, *100*, 10658−10663.

(19) Allen, M. P.; Tildesley, D. J. *Computer Simulation of Liquids*; van Gunsteren, W. F., Weiner, P. K., Ed.; Clarendon Press: Oxford, 1987.

(20) Meyer, M.; Mareschal, M.; Hayoun, M. *J. Chem. Phys.* **1988**, *89*, 1067−1073.

(21) Gao, J.; Jorgensen, W. L. *J. Phys. Chem.* **1988**, *92*, 5813−5822. Benjamin, I. *J. Chem. Phys.* **1992**, *97*, 1432−1445. van Buuren, A. R.; Marrink, S.-J.; Berendsen, J. C. *J. Phys. Chem.* **1993**, *97*, 9206−9212. Linse, P. *J. Chem. Phys.* **1987**, *86*, 4177−4187.

(22) Smit, B. NATO ASI Serv., Ser. C. (*Comput. Simul. Chem. Phys.* **1993**, *398*, 461−472. Smit, B.; Esselink, K.; Hilbers, P. A. J.; van Os, N. M.; Rupert, L. A. M.; Szleifer, I. *Langmuir* **1993**, *9*, 9−11. Esslink, K.; Hilbers, P. A. J.; van Os, N. M.; Smit, B.; Karaborni, S. *Colloids Surf. A* **1994**, *91*, 155−167. Marrink, S.-J.; Berendsen, H. J.-C. *J. Phys. Chem.* **1994**, *98*, 4155−4168. Wilson, M. A.; Pohorille, A. *J. Am. Chem. Soc.* **1994**, *116*, 1490−1501.

(23) Wilson, M. A.; Pohorille, A.; Pratt, L. R. *Chem. Phys.* **1989**, *129*, 209−212. Pohorille, A.; Cieplak, P.; Wilson, M. A. *Chem. Phys.* **1996**, *204*, 337−345. Benjamin, I. *J. Chem. Phys.* **1991**, *95*, 3698−3709.

(24) Wilson, M. A.; Pohorille, A. *J. Chem. Phys.* **1991**, *95*, 6005−6013.

(25) Pohorille, A.; Benjamin, I. *J. Chem. Phys.* **1991**, *94*, 5599−5605. Pohorille, A.; Benjamin, I. *J. Phys. Chem.* **1993**, *97*, 2664−2670.

(26) Chipot, C.; Wilson, M. A.; Pohorille, A. *J. Phys. Chem. B* **1997**, *101*, 782−791.

(27) Guba, W.; Haessner, R.; Breipohl, G.; Henke, S.; Knolle, J.; Sandagada, V.; Kessler, H. *J. Am. Chem. Soc.* **1994**, *116*, 7532−7540. Guba, W.; Kessler, H. *J. Phys. Chem.* **1994**, *98*, 23−27.

(28) Torrie, G. M.; Valleau, J. P. *J. Electroanal. Chem.* **1986**, *106*, 69−79.

(29) Benjamin, I. *J. Chem. Phys* **1992**, *96*, 577−585. Benjamin, I. *Science* **1993**, *261*, 1558−1560. Schweighofer, K. J.; Benjamin, I. *J. Phys. Chem.* **1995**, *99*, 9974−9985. Benjamin, I. *Chem. Rev. (Washington, D.C.)* **1996**, *96*, 1449−1475. Benjamin, I. *Acc. Chem. Res* **1995**, *28*, 233−239.

(30) Wipff, G.; Engler, E.; Guilbaud, P.; Lauterbach, M.; Troxler, L.; Varnek, A. *New J. Chem.* **1996**, *20*, 403−417.

(31) Wipff, G.; Lauterbach, M. *Supramol. Chem.* **1995**, *6*, 187−207.

(32) Lauterbach, M.; Wipff, G. In *Physical Supramolecular Chemistry*; Echegoyen, L., Kaifer, A., Ed.; Kluwer Academic Publishers: Dordrecht, 1999; pp 65−102.

(33) Varnek, A.; Sirlin, C.; Wipff, G. In Crystallography of Supramolecular Compounds; **1995**, Tsoucaris, G., Ed.; Kluwer Academic Publishers: Dordrecht, 1995; pp 67−100.

(34) Varnek, A.; Wipff, G. *J. Comput. Chem.* **1996**, *17*, 1520−1531.

(35) Guilbaud, P.; Wipff, G. *New J. Chem.* **1996**, *20*, 631−642. Beudaert, P.; Lamare, V.; Dozol, J.-F.; Troxler, L.; Wipff, G. *Solvent Extr. Ion Exch.*

(36) Varnek, A.; Troxler, L.; Wipff, G. *Chem. Eur. J.* **1997**, *3*, 552−560.

(37) Ungaro, R.; Casnati, A.; Ugozzoli, F.; Pochini, A.; Dozol, J.-F.; Hill, C.; Rouquette, H. *Angew. Chem., Int. Ed. Engl.* **1994**, *33*, 1506−1509. Ungaro, R.; Arduini, A.; Casnati, A.; Ori, O.; Pochini, A.; Ugozzoli, F. In *Computational Approaches in Supramolecular Chemistry*; Wipff, G., Ed.; Kluwer Academic Publishers: Dordrecht, 1994; pp 277−300. Casnati, A.; Pochini, A.; Ungaro, R.; Ugozzoli, F.; Arnaud, F.; Fanni, S.; Schwing-Weil, M.-J.; Egberink, R. J. M.; Reinhoudt, D. N. *J. Am. Chem. Soc.* **1995**, *117*, 2767−2777.

(38) Beveridge, D. L.; Di Capua, F. M. *Annu. Rev. Biophys. Biophys. Chem.* **1989**, *18*, 431−492. Jorgensen, W. L. *Acc. Chem. Res* **1989**, *22*, 184−189.

(39) Koenig, K. E.; Lein, G. M.; Stuckler, P.; Kaneda, T.; Cram, D. J. *J. Am. Chem. Soc.* **1979**, *101*, 3553.

(40) Wipff, G.; Troxler, L. *AIP Conference Proceedings 330*, Bernardi F., Rivail, J.-L., Ed.; AIP Press: Woodbury, NY, 1995, 325−336.

(41) Pearlman, D. A.; Case, D. A.; Cadwell, J. C.; Seibel, G. L.; Singh, U. C.; Weiner, P.; Kollman, P. A. *AMBER 4*; University of California: San Francisco, 1991.

(42) Weiner, S. J.; Kollman, P. A.; Nguyen, D. T.; Case, D. A. *J. Comput. Chem.* **1986**, *7*, 230−252. Cornell, W. D.; Cieplak, P.; Bayly, C. I.; Gould, I. R.; Merz, K. M.; Ferguson, D. M.; Spellmeyer, D. C.; Fox, T.; Caldwell, J. W.; Kollman, P. A. *J. Am. Chem. Soc.* **1995**, *117*, 5179−5197.

(43) Jorgensen, W. L.; Chandrasekhar, J.; Madura, J. D. *J. Chem. Phys.* **1983**, *79*, 926−936.

(44) Jorgensen, W. L.; Briggs, J. M.; Contreras, M. L. *J. Phys. Chem.* **1990**, *94*, 1683−1686.

(45) Riddick, J. A.; Bunger, W. B.; Sakano, T. K. *Organic Solvents: Physical Properties and Methods of Purification*; Wiley: New York, 1981.

(46) Berendsen, H. J. C.; Postma, J. P. M.; van Gunsteren, W. F.; Di Nola, A. *J. Chem. Phys.* **1984**, *81*, 3684−3690.

(47) Engler, E.; Wipff, G. *Unpublished* manuscript.

(48) Engler, E.; Wipff, G. In *Crystallography of Supramolecular Compounds*"; Tsoucaris, G., Ed.; Kluwer: Dordrecht, 1996; pp 471−476.

(49) Hill, C.; Dozol, J.-F.; Lamare, V.; Rouquette, H.; Tournois, B.; Vicens, J.; Asfari, Z.; Bressot, C.; Ungaro, R.; Casnati, In *Calixarenes 50th Anniversary*: *Commemorative Issue*; Vicens, J., Asfari, Z. Harrowfield, J., Ed.; Kluwer Academic Publishers: Dordrecht, 1995. Asfari, Z.; Bressot, C.; Vicens, J.; Hill, C.; Dozol, J.-F.; Rouquette, H.; Eymard, S.; Lamare, V.; Tournois, B. In *Chemical Separations with Liquid Membranes*, Bartsch, R. A., Way, J. D., Ed.; American Chemical Society, Washington, DC, 1996; 376−390. Asfari, Z.; Naumann, C.; Vicens, J.; Nierlich, M.; Thuéry, P.; Bressot, C.; Lamare, V.; Dozol, J.-F. *New. J. Chem.* **1996**, *20*, 1183−1194.

(50) Guillot, B.; Guissani, Y.; Bratos, S. *J. Chem. Phys.* **1991**, *95*, 3643−3648. Wallqvist, A. *J. Phys. Chem.* **1991**, *95*, 8921−8927. Blokzijl, W.; Engberts, J. B. F. N. *Angew. Chem., Int. Ed. Engl.* **1993**, *32*, 1545−1579. Pohorille, A.; Pratt, L. R. *J. Am. Chem. Soc.* **1990**, *112*, 5066−5074. Pierotti, R. A. *Chem. Rev. (Washington, D.C.)* **1976**, *76*, 717−726. Prévost, M.; Oliveira, I. T.; Kocher, J. P.; Wodak, S. J. *J. Phys. Chem.* **1996**, *100*, 2738−2743.

(51) Vandegrift, G. F.; Horwitz, E. P. *J. Inorg. Nucl. Chem.* **1977**, *39*, 1425−1432. Kalina, D. G.; Horwitz, E. P.; Kaplan, L.; Muscatello, A. C. *Sep. Sci. Technol.* **1981**, *16*, 1127. Lin, S.-Y.; Lin, L.-W.; Chang, H.-C.; Ku, Y. *J. Phys. Chem.* **1996**, *100*, 16678−16684.

(52) Cross, J. *Non −Ionic surfactants. Chemical Analysis*; M. Dekker, Inc.: New York, 1987. Aveyard, R.; Vincent, B. *Prog. Surf. Science* **1977**, *8*, 59−102.

(53) Sagert, N. H.; Lee, W.; Quinn, M. J. *Can. J. Chem.* **1979**, *57*, 1218−1223.

(54) Chifu, E.; Andrei, Z.; Tomoaia, M. *Anal. Chim. (Rome)* **1974**, *64*, 869−871. Tomoaia, M.; Andrei, Z.; Chifu, E. *Rev. Roum. Chim.* **1973**, *18*, 1547.

(55) Danesi, P. R.; Chiarizia, R.; Pizzichini, M.; Saltelli, A. *J. Inorg. Nucl. Chem.* **1978**, *40*, 1119−1123.

(56) Popov, A. N. In *The Interface Structure and Electrochemical Processes at the Boundary Between two Immiscible Liquids*, Kazarinov, V. E., Ed.; Springer-Verlag: Berlin, 1987; pp 179−205.

(57) Charewicz, W. A.; Radzicka, W.; Strzelbicki, J. *J. Colloid Interface Sci.* **1980**, *76*, 290−297.

(58) Ishikawa, Y.; Kunitake, T.; Matsuda, T.; Otsuka, T.; Shinkai, S. *J. Chem. Soc., Chem. Commun.* **1989**, 736−737. Dei, L.; Casnati, A.; Nostro, P. L.; Baglioni, P. *Langmuir* **1995**, *11*, 1268−1272. Nostro, P. L.; Casnati, A.; Bossoletti, L.; Dei, L.; Baglioni, P. *Colloids Surf., A* **1996**, *116*, 203−209.

(59) Vandegrift, G. F.; Delphin, W. H. *J. Inorg. Nucl. Chem.* **1980**, *42*, 1359−1361.

(60) Kuo, P.-L.; Ikeda, I.; Okahara, M. *Tenside, Surfactants, Deterg.* **1982**, *19*, 204.

(61) Tamburello-Luca, A. A.; Hébert, P.; Brevet, P. F.; Girault, H. G. *J. Chem. Soc., Faraday Trans* **1996**, *92*, 3079−3085.

(62) Carlà, M.; C. M. C. Gambi; Baglioni, P. *J. Phys. Chem.* **1996**, *100*, 11067−11071.

(63) Fyles, T. M.; Malid-Diemer, V. A.; McGavin, C. A.; Whitfield, D. M. *Can. J. Chem.* **1982**, *60*, 2259−2267. Fyles, T. M. *J. Membr. Sci.* **1985**, *24*, 229−243. See also ref 5.

(64) Yoshida, Z.; Kihara, S. *J. Electroanal. Chem.* **1987**, *227*, 171−181. Yoshida, S.; Okawa, Y.; Watanabe, T.; Inokuma, S.; Kuwamura, T. *Chem. Lett.* **1989**, 243−246.

(65) (a) Yoshida, Z.; Freiser, H. *J. Electroanal. Chem.* **1984**, *179*, 31−39. (b) Vanysek, P.; Ruth, W.; Koryta, J. *J. Electroanal. Chem.* **1983**, *148*, 117−121. Hofmanova, A.; Hung, L. Q.; Khalil, W. *J. Electroanal. Chem.* **1982**, *135*, 257−264.

(66) Koryta, J. *Electrochim. Acta* **1984**, *29*, 445.

(67) Homolka, D.; Hung, L. G.; Hofmanova, A.; Khalif, M. W.; Koryta, J.; Marecek, V.; Samec, Z.; Sen, S. K.; Vanysek, P.; Weber, J.; Brezina, M.; Janda, M.; Stibor, I. *Anal. Chem.* **1980**, *52*, 1606. Sinru, L.; Zaofan, Z.; Freiser, H. *J. Electroanal. Chem.* **1986**, *210*, 137−146. Sinru, L.; Freiser, H. *J. Electroanal. Chem.* **1985**, *191*, 437−439. Beattie, P. D.; Delay, A.; Girault, H. H. *Electrochim. Acta* **1995**, *40*, 2961−2969. Beattie, P. D.; Delay, A.; Girault, H. H. *J. Electroanal. Chem.* **1995**, *380*, 167−175.

(68) Lamb, J. D.; Christensen, J. J.; Izatt, S. R.; Bedke, K.; Astin, M. S.; Izatt, R. M. *J. Am. Chem. Soc.* **1980**, *102*, 3399−3403.

(69) Abraham, M. H.; Liszi, J. *J. Inorg. Nucl. Chem.* **1981**, *43*, 143−151.

(70) Frumkin, A. *Z. Phys. Chem.* **1924**, *109*, 34. Randles, J. E. *Discuss. Faraday Soc.* **1957**, *24*, 194−199.

(71) Jarvis, N. L.; Scheiman, M. A. *J. Phys. Chem.* **1968**, *72*, 74.

(72) Hofmeister, F. *Naunyn-Schmiedeberg,s Arch. für Exp. Pathol. Pharmakol.* **1888**, *24*, 247−260. Collins, K. D.; Washabaugh, M. W. *Quater. Rev. Biophys.* **1985**, *18*, 323−422.

(73) Goard, A. K. *J. Chem. Soc.* **1925**, *127*, 2451−2458.

(74) Fan, W.; Tsai, R.-S.; El Tayar, N.; Carrupt, P.-A.; Testa, B. *J. Phys. Chem.* **1994**, *98*, 329−333. Fan, W.; El Tayer, N.; Testa, B.; Kier, L. B. *J. Phys. Chem.* **1990**, *94*, 4764. Tsai, R.-S.; Fan, W.; El Tayar, N.; Carrupt, P. A.; Testa, B.; Kier, L. B. *J. Am. Chem. Soc.* **1993**, *115*, 9632−9639.

(75) Watarai, H.; Sasaki, K.; Takahashi, K.; Murakami, J. *Talanta* **1995**, *42*, 1691−1700.

(76) Chang, T.-M.; Peterson, K. A.; Dang, L. X. *J. Chem. Phys.* **1995**, *103*, 7502−7513. Dang, L. X.; Rice, J. E.; Caldwell, J.; Kollman, P. A. *J. Am. Chem. Soc.* **1991**, *113*, 2481−2486.

(77) Smith, P. E.; van Gunsteren, W. F. In Computer Simulations of Biomolecular Systems; van Gunsteren, W. F.; Weiner, P. K. Wilkinson, A. J. Ed.; ESCOM: Leiden, 1993; pp 182−212. Smith, P. E.; Pettitt, B. M. *J. Chem. Phys.* **1991**, *95*, 8430−8441. Kollman, P. A.; Chipot, C.; Millot, C.; Maigret, B. *J. Chem. Phys.* **1994**, *101*, 7953−7962. Bartolotti, L. J.; Pedersen, L. G.; Charifson, P. S. *J. Comput. Chem.* **1991**, *12*, 1125−1128. Madura, J. D.; Pettitt, B. M. *Chem. Phys. Lett.* **1988**, *150*, 105−108. York, D. M.; Darden, T. A.; Pedersen, L. G. *J. Chem. Phys.* **1993**, *99*, 8345−8348. Daura, X.; Hünenberger, P. H.; Mark, A. E.; Querol, E.; Avilés, F. X.; van Gunsteren, W. F. *J. Am. Chem. Soc.* **1996**, *118*, 6285−6294. Brooks III, C. L.; Pettitt, B. M.; Karplus, M. *J. Chem. Phys.* **1985**, *83*, 5897.

(78) Muzet, N.; Wipff, G. Unpublished results.

(79) Muzet, N.; Troxler, L.; Wipff, G. Proceedings of the 25th International Conference on Solution Chemistry; Vichy, 1997 (IUPAC) conference.

(80) Sokhan, V. P.; Tildesley, D. *J. Faraday Discuss.* **1996**, *104*, 193.

(81) The role of concentration has recently investigated computationally on the (18-crown-6 $K^+Pic^-)_n$ system at the water chloroform interface, simulated for 1 ns (Troxler, L.; Wipff, G. *Anal. Sci.* in press). With $n = 1$,

the complex remained at interface during the whole simulation. With $n = 6$, a equilibrium situation was found where some complexes decomplexed, one was extracted to chloroform, and others remained at the interface.

(82) We performed recently a FEP study on the LNa^+/LCs^+ complexes at the water−chloroform interface and found a preference for Cs^+ complexation.[78]

(83) Montserrat, K.; Graetzel, M.; Tundo, P. *J. Am. Chem. Soc.* **1980**, *102*, 2, 5527−5529. Liu, Y. C.; Baglioni, P.; Texeira, J.; Chen, S. H. *J. Phys. Chem.* **1994**, *98*, 10208−10215. Ginley, M.; Henriksson, U.; Li, P. *J. Phys. Chem.* **1990**, *94*, 4644−4648. Evans, D. F.; Evans, J. B.; Sen, R.; Warr, G. G. *J. Phys. Chem.* **1988**, *92*, 784−790. Ginley, M.; Henriksson, U. *J. Colloid Interface Sci.* **1992**, *150*, 281−284.

(84) Honig, B. H.; Hubbel, W. L.; Flewelling, R. F. *Annu. Rev. Biophys. Biophys. Chem.* **1986**, *15*, 163. Gennis, R. B. Ed. *Biomembranes*; Springer: New York, 1989. Shao, Y.; Girault, H. H. *J. Electroanal. Chem.* **1990**, *282*, 59.